Duality in topological superconductors and topological ferromagnetic insulators in a honeycomb lattice

Shin-Ming Huang[1], Wei-Feng Tsai[2], Chung-Hou Chung[3,4], and Chung-Yu Mou[1,4,5]
[1] *Department of Physics, National Tsing Hua University, Hsinchu 30043, Taiwan, 300, R.O.C.*
[2] *Department of Physics, National Sun Yat-Sen University, Kaohsiung, Taiwan, R.O.C.*
[3] *Electrophysics Department, National Chiao-Tung University, Hsinchu, Taiwan, R.O.C.*
[4] *Physics Division, National Center for Theoretical Sciences, P.O.Box 2-131, Hsinchu, Taiwan, R.O.C.*
[5] *Department of Physics, National Tsing Hua University, Hsinchu 30043, Taiwan, 300, R.O.C. and*
[7] *Institute of Physics, Academia Sinica, Nankang, Taiwan, R.O.C.*
(Dated: January 7, 2016)

The ground state of large Hubbard U limit of a honeycomb lattice near half-filling is known to be a singlet $d+id$-wave superconductor. It is also known that this $d+id$ superconductor exhibits a chiral $p+ip$ pairing locally at the Dirac cone, characterized by a $2\mathbb{Z}$ topological invariant. By constructing a dual transformation, we demonstrate that this $2\mathbb{Z}$ topological superconductor is equivalent to a collection of two topological ferromagnetic insulators. As a result of the duality, the topology of the electronic structures for a $d+id$ superconductor is controllable via the change of the chemical potential by tuning the gate voltage. In particular, instead of being always a chiral superconductor, we find that the $d+id$ superconductor undergoes a topological phase transition from a chiral superconductor to a quasi-helical superconductor as the gap amplitude or the chemical potential decreases. The quasi-helical superconducting phase is found to be characterized by a topological invariant in the pseudo-spin charge sector with vanishing both the Chern number and the spin Chern number. We further elucidate the topological phase transition by analyzing the relationship between the topological invariant and the rotation symmetry. Due to the angular momentum carried by the gap function and spin-orbit interactions, we show that by placing $d+id$ superconductors in proximity to ferromagnets, varieties of chiral superconducting phases characterized by higher Chern numbers can be accessed, providing a new platform for hosting large numbers of Majorana modes at edges.

I. INTRODUCTION

A $\mathbb{Z}$ topological insulator in two dimensions, also called a Chern insulator, characterized by the Chern number, is an electronic system with broken time-reversal symmetry (TRS), showing a quantized Hall conductivity[1] and protected gapless edge modes.[2,3] An example is the quantum anomalous Hall (QAH) effect, being achieved by a magnetic exchange field.[4,5] After the discovery of the $\mathbb{Z}_2$ quantum spin Hall (QSH) insulator,[6–11] it is realized that symmetries play important roles in classifying a topological state. According to the AZ-classification scheme by TRS, particle-hole symmetry (PHS), and chiral symmetry,[12,13] topological insulators and superconductors in different non-spatial symmetry classes belong to different category and are not connected in topology.[14–16] From symmetry point of view on the energy spectrum, however, superconductors have energy gaps and can be considered as an insulator with conduction and valence bands related by the particle-hole symmetry. It is therefore interesting to explore possible connections of superconductors and insulators in the topology of electronic structures. Such connection can be useful in help searching possible realizations of Majorana modes in superconductors.

In the past, the investigation on topological superconductors had been mostly focusing on the triplet pairing superconductors with TRS breaking. These topological superconductors host chiral Majorana fermions at edges but there are very few confirmed observations.[17–20] Until recently, thanks to the seminal work by Fu and Kane,[21,22] it is now realized that the proximity of a topological insulator to a singlet s-wave superconductor provides an alternative way to topological superconductors. The combined effect of s-wave and the spin-orbit coupling (SOC) plays an important role in hosting Majorana fermions. In this case, the most general topological superconductors are time-reversal invariant helical superconductors (HSCs), characterized by a $\mathbb{Z}_2$ topological invariant.[23–25] More recently, possible solutions of spin-singlet topological superconductors via spontaneously TRS breaking are proposed.[26–29] In particular, the ground state for electrons on the honeycomb lattice in the large Hubbard U limit are shown to be of chiral d-wave pairing symmetry, $d_{x^2-y^2}+id_{xy}$ $(d+id)$,[30] which indicates that the honeycomb lattice might be a good platform to host chiral Majorana modes.

In this paper, we explore the topology of electronic structures for $d+id$ -wave superconductivity in a honeycomb lattice. We first demonstrate that the electronic structures of a $d+id$ superconductor and a ferromagnetic insulator on a honeycomb lattice are interchanged under a dual transformation. As a result of the duality, the topology of the electronic structures for a $d+id$ superconductor is equivalent to that of a ferromagnetic insulator. The idea of a dual transformation from an s-wave superconductor with the Rashba SOC to a p-wave superconductor was proposed before,[31] but the dual system was obscure in physical meaning. The duality in our models is

between two realistic ones and indicates equivalent topological structures underlying. In the ferromagnetic insulator, QAH and spin Chern insulating (SCI)/QSH phases can be found. QAH and SCI/QSH phases are characterized by a non-vanishing Chern number and a spin Chern number, respectively. The spin Chern number is an alternative way to characterize the $\mathbb{Z}_2$ QSH insulator,[32] which originates from the intuition that when the fiber bundles of filled states are projected into spin-up and spin-down sectors the nontrivial topological structure can be found in each spin section.[33] The spin Chern number is confirmed to be a robust topological invariant against disorder or spin-nonconserving interactions (such as Rashba SOC). Unlike the $\mathbb{Z}_2$ invariant, the spin Chern number can be generalized to the case when TRS is broken as long as the band gap remains open to preserve a finite spin polarization.[32–35] With the aid of the duality, a phase analogous to SCI/QSH, termed as quasi-HSC, is found in $d+id$ superconductors. Here "quasi" indicates that there is no exact time-reversal partner between counter-propagating edge modes. The quasi-HSC phase has no spin Chern number and is characterized by a pseudo-spin Chern number in the charge sector not in the spin sector. As the topological phase undergoes a transition to a chiral superconductor (CSC) for larger gap amplitudes or the chemical potentials, its topology is described by the Chern number and it is realized as a combination of two QAH systems with a charge conjugate relation. Furthermore, We elucidate the topological phase by analyzing the relationship between the topological invariant and the rotation symmetry associated with the angular momentum carried by the gap function and SOC. When the $d+id$ superconductor is in proximity to a ferromagnet, the superconducting state coexists with ferromagnetism. We find that varieties of chiral superconducting phases characterized by higher Chern numbers can be accessed, which provides a new platform for hosting large numbers of Majorana modes at edges.

II. THEORETICAL MODELS

In this section, we start by considering the topological ferromagnetic insulator in Sec. II A. The phase diagram will be constructed. The spin-singlet $d+id$-wave topological superconductor will be investigate in Sec. II B. The duality relation with the topological ferromagnetic insulator will be clarified. Finally, in Sec. II C, we combine both models by considering the situation when the $d+id$ superconductor is in proximity to a ferromagnet. The topological phase diagram for the case when the superconductivity coexists with ferromagnetism is constructed. The effect of duality on the phase diagram and the relation to the rotation symmetry will be given.

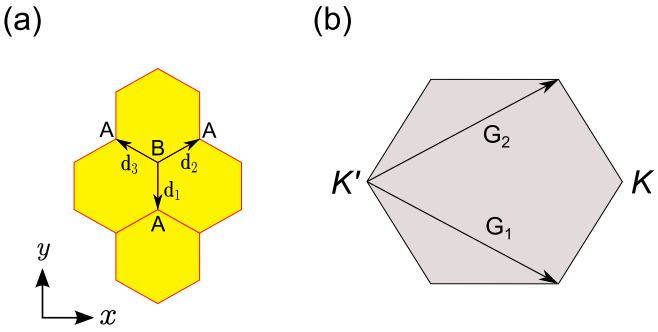

FIG. 1. (Color online) (a) Three nearest neighbour vectors $\mathbf{d}_{1,2,3}$ and coordinates in a honeycomb lattice. (b) Brillouin zone and reciprocal lattice vectors, $\mathbf{G}_1$ and $\mathbf{G}_2$

A. Class A insulator

We start by considering the Kane-Mele model in the presence of the exchange field $-M$

$$\hat{H}_{\rm FM} = -t\sum_{\langle i,j\rangle} c_i^\dagger c_j + i\frac{\lambda_{\rm SO}}{3\sqrt{3}}\sum_{\langle\langle i,j\rangle\rangle}\nu_{ij}c_i^\dagger\sigma_z c_j \qquad (1)$$
$$+i\frac{2\lambda_{\rm R}}{3}\sum_{\langle i,j\rangle} c_i^\dagger\hat{z}\cdot\left(\sigma\times\hat{\mathbf{d}}_{ij}\right)c_j - M\sum_i c_i^\dagger\sigma_z c_i.$$

Here the first term describes the hopping, the second term is the intrinsic SOC, the third one is the Rashba SOC, and the last term is the exchange field. $c_i^\dagger = \left(c_{i\uparrow}^\dagger, c_{i\downarrow}^\dagger\right)$ is the electron creation operator on site i, σ is the Pauli matrix, and $\langle i,j\rangle$ and $\langle\langle i,j\rangle\rangle$ denote i and j being nearest-neighbor (NN) and next-nearest-neighbor (NNN) sites, respectively. $\hat{\mathbf{d}}_{ij} = \mathbf{d}_{ij}/|\mathbf{d}_{ij}|$ are unit vectors connecting site j and i. Three NN vectors $\mathbf{d}_l$ $(l=1,2,3)$ along with the coordinates are shown in Fig. 1. $\nu_{ij} = \mathrm{sgn}(\hat{z}\cdot\mathbf{d}_{kj}\times\mathbf{d}_{ik}) = \pm 1$ for ij being connected by $\mathbf{d}_{kj}$ and $\mathbf{d}_{ik}$.

After the Fourier transformation, the Bloch Hamiltonian becomes

$$\mathcal{H}_{\rm FM}(\mathbf{k}) = \begin{pmatrix} \Lambda_{\mathbf{k}}-M & T_{\mathbf{k}} & 0 & R_{\mathbf{k}} \\ T_{\mathbf{k}}^* & -\Lambda_{\mathbf{k}}-M & -R_{-\mathbf{k}} & 0 \\ 0 & -R_{-\mathbf{k}}^* & -\Lambda_{\mathbf{k}}+M & T_{\mathbf{k}} \\ R_{\mathbf{k}}^* & 0 & T_{\mathbf{k}}^* & \Lambda_{\mathbf{k}}+M \end{pmatrix} \qquad (2)$$

in the basis $c_{\rm FM}(\mathbf{k}) = \left(\begin{array}{cccc} c_{A\mathbf{k}\uparrow} & c_{B\mathbf{k}\uparrow} & c_{A\mathbf{k}\downarrow} & c_{B\mathbf{k}\downarrow}\end{array}\right)^T$, with

$$T_{\mathbf{k}} = -t\sum_l e^{-i\mathbf{k}\cdot\mathbf{d}_l}, \qquad (3)$$

$$\Lambda_{\mathbf{k}} = \frac{2\lambda_{\rm SO}}{3\sqrt{3}}\sum_{l\ (\mathbf{d}_4=\mathbf{d}_1)}\sin\mathbf{k}\cdot\left(\mathbf{d}_l-\mathbf{d}_{l+1}\right), \qquad (4)$$

$$R_{\mathbf{k}} = -\frac{2\lambda_{\rm R}}{3}\sum_l e^{-i\theta_l}e^{-i\mathbf{k}\cdot\mathbf{d}_l}, \qquad (5)$$

where θ_l is the polar angle of the vector $\mathbf{d}_l$. We will

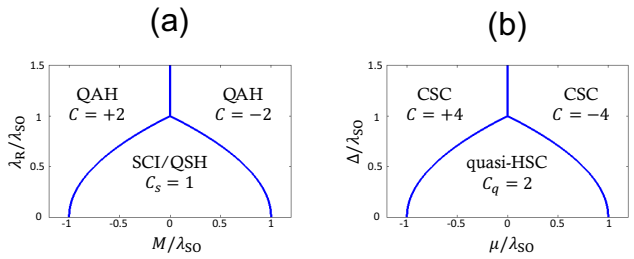

FIG. 2. (Color online) (a) Phase diagram for the ferromagnetic system in Eq. (1). QAH and SCI/QSH denote phases of quantum anomalous Hall insulator and spin Chern insulator/quantum spin Hall insulator, which are dubbed by nonzero Chern number C and spin Chern number $C_s = (C_\uparrow - C_\downarrow)/2$, respectively. (b) The phase diagram for the superconducting state in Eq. (14). Similar to (a) with substitutions: $M \to \mu$, $\lambda_{\rm R} \to \Delta$, doubled Chern numbers, $C = \pm 2 \to C = \pm 4$, and $C_s = 1 \to C_q = 2$ (see text), and CSC/quasi-HSC (chiral/quasi-helical superconductor) in place of QAH/SCI. Note that for the QAH and CSC phases, one requires $\lambda_{\rm R} \neq 0$ and $\Delta \neq 0$, respectively.

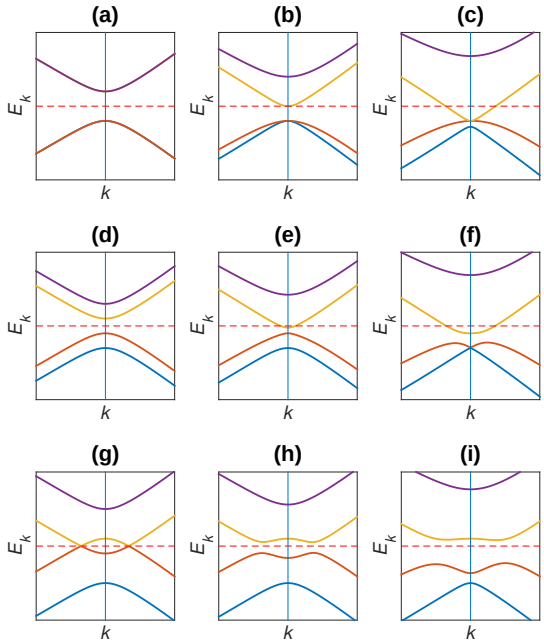

FIG. 3. (Color online) Energy dispersion around the K point (vertical line) for the topological insulator with ferromagnetism described by Eq. (1). Different combinations of M and $\lambda_{\rm R}$ are given. M increases from top to bottom; $M/\lambda_{\rm SO} = 0$ [(a), (b), (c)], 0.5 [(d), (e), (f)], and 1.5 [(g), (h), (i)], respectively. On the other hand, $\lambda_{\rm R}$ increases from left to right; $\lambda_{\rm R}/\lambda_{\rm SO} = 0$ [(a), (d), (g)], 0.5 [(b), (e), (h)], and 1.2 [(c), (f), (i)], respectively. The horizontal dashed line denotes zero energy as the unbiased chemical potential. If one can shift the chemical potential within the gap between middle two bands, topological phases are achieved: (a) and (b) are in the QSH phase. (d) and (e) are in the SCI phase. (c) and (g) are in the critical semimetal phase, preparing for entering the QAH phase, and (f), (h), (i) are in the QAH phase.

set the lattice constant and Planck constant as unity, $\hbar = a = 1$.

The topological phases of the Kane-Mele model have been understood and are summarized in Fig. 2(a). When $M = 0$ and $\lambda_{\rm SO} > |\lambda_{\rm R}|$ (assume $\lambda_{\rm SO} > 0$), the low-energy physics is described by a massive Dirac fermion (and its time-reversal partner with an opposite mass) at K and K' points where Berry phases π $(-\pi)$ are underlying. This is a QSH phase characterized by a $\mathbb{Z}_2$ topological invariant. When $M \neq 0$ and TRS is broken, the QSH phase is replaced by the SCI phase when $\lambda_{\rm SO} > 0$. In this case, even though one still gets counter-propagating edge states, these edges states are not robust and can be gapped under perturbations.[35] However, the spin Chern number is still well-defined[33] and is intact.[34] The robustness of the value for the spin Chern number is due to the spin gap, associated with the band gap, that two occupied states remain carrying definite opposite spin projections as TRS preserves.[35] The topological phase transition happens at the closing of the band gap, given by

$$|M| = \left(\lambda_{\rm SO}^2 - \lambda_{\rm R}^2\right)/\lambda_{\rm SO}. \tag{6}$$

Over the boundary in Eq. (6) with $\lambda_{\rm R}$ and M both finite, the system enters the QAH phase with Chern number $C = \pm 2$.[36]

To elucidate the topological phase transition more clearly, the band structures near K for different cases of $\lambda_{\rm R}$ and M are shown in Fig. 3 with $\lambda_{\rm R}/\lambda_{\rm SO} = 0$, 0.5, 1.2 from left to right columns and $M/\lambda_{\rm SO} = 0$, 0.5, 1.5 from top to bottom rows. At $\lambda_{\rm R} = M = 0$, Fig. 3(a), bands are spin-degenerate and are separated by a gap of $2\lambda_{\rm SO}$. Non-vanishing $\lambda_{\rm R}$ and/or M lifts the spin degeneracy and brings the conduction and the valence bands approaching to each other. The resulting phase is an SCI phase. As a result, the band gap prevents the band inversion to occur immediately and thus protects the resulting SCI phase. Once $\lambda_{\rm R}$ and M terms overcome the gap by $\lambda_{\rm SO}$, due to that $\lambda_{\rm R}$ and M terms anti-commute, two bands must anti-cross and exchange the Chern number, resulting in a QAH phase.

We now illustrate the change of the Chern number from the point of view of exchanging rotation eigenvalues. In an insulator with point group symmetries, the eigenvalues of symmetry operators at high-symmetry points of the ground state determine the Chern number up to a multiple of n in the presence of n-fold axis. By Ref. [37], a three-fold-symmetric insulator as our system gives

$$e^{-i2\pi C/3} = \prod_{i\in {\rm occ.}} \eta_i(\Gamma)\eta_i(K)\eta_i(K'), \tag{7}$$

where $\eta_i(\mathbf{k})$ is the eigenvalues of the three-fold rotation. Since the band inversion happens at K and K', we can study the change of the Chern number by the change of rotation eigenvalues at K and K'. The eigenenergies of the Bloch Hamiltonian at K and K', Eq. (2), are

$$\begin{array}{l} E_1 = -\lambda_{\rm SO} - M, \\ E_2 = -\lambda_{\rm SO} + M, \\ E_3 = \lambda_{\rm SO} - \sqrt{M^2 + 4\lambda_{\rm R}^2}, \\ E_4 = \lambda_{\rm SO} + \sqrt{M^2 + 4\lambda_{\rm R}^2}. \end{array} \tag{8}$$

Here the rotation eigenvalues of these four states at K are given by

$$\begin{array}{l} \eta_1^K = e^{i\pi/3}, \\ \eta_2^K = e^{-i3\pi/3}, \\ \eta_3^K = e^{-i\pi/3}, \\ \eta_4^K = e^{-i\pi/3}, \end{array} \tag{9}$$

respectively, while for the K' point, the rotation eigenvalues of these four eigenenergies are

$$\begin{array}{l} \eta_1^{K'} = e^{i3\pi/3}, \\ \eta_2^{K'} = e^{-i\pi/3}, \\ \eta_3^{K'} = e^{i\pi/3}, \\ \eta_4^{K'} = e^{i\pi/3}, \end{array} \tag{10}$$

respectively. Detailed derivation of rotation eigenvalues can be found in Appendix A. Consider the case of $M > 0$. The band inversion happens between the band-2 (eigenenergy E_2) and the band-3 (E_3) at the critical point specified by Eq. (6). Hence the rotation eigenvalue changes by $e^{i2\pi/3}$ at K point. Meanwhile, the rotation eigenvalue also changes by $e^{i2\pi/3}$ at K'. The total change of the rotation eigenvalue by $e^{i4\pi/3}$ indicates that the change of the Chern number is -2 ($+1$ is ruled out because the band inversion occurs at two points: both at K and K' points). On the other hand, for the case of $M < 0$, the band inversion happens between the band-1 and the band-3, reflecting in the change of the Chern number by 2. A consistent explanation has been given by referring to Fig. 2(a).

B. $d + id$ superconductor

In this section, we examine the topology of the electronic structures for the singlet $d + id$ superconducting state. We start by first analyzing a generic feature of energy spectrum for quasi-particles in the singlet superconductors with spin S_z conservation. The general BdG Hamiltonian for quasi-particles for singlet superconductivity can be written as

$$\hat{H} = \frac{1}{2}\sum_{\mathbf{k}} \phi_{\mathbf{k}}^\dagger \mathcal{H}_{\mathbf{k}} \phi_{\mathbf{k}}, \tag{11}$$

where $\phi_{\mathbf{k}} = (\ c_{\mathbf{k}\uparrow}\ \ c_{\mathbf{k}\downarrow}\ \ c_{-\mathbf{k}\uparrow}^\dagger\ \ c_{-\mathbf{k}\downarrow}^\dagger\ )^T$ with $c_{\mathbf{k}\sigma}(c_{\mathbf{k}\sigma}^\dagger)$ being possibly a multi-component vector by including orbital degrees of freedom. For singlet superconductivity with S_z being conserved, the Bloch Hamiltonian is generally given by

$$\mathcal{H}_{\mathbf{k}} = \begin{pmatrix} \xi_{\mathbf{k}\uparrow} & 0 & 0 & \Delta_{\mathbf{k}} \\ 0 & \xi_{\mathbf{k}\downarrow} & -\Delta_{\mathbf{k}} & 0 \\ 0 & -\Delta_{\mathbf{k}}^\dagger & -\xi_{-\mathbf{k}\uparrow}^T & 0 \\ \Delta_{\mathbf{k}}^\dagger & 0 & 0 & -\xi_{-\mathbf{k}\downarrow}^T \end{pmatrix}, \tag{12}$$

where $\xi_{\mathbf{k}\sigma}$ and $\Delta_{\mathbf{k}}$ can be numbers or matrices and $\Delta_{-\mathbf{k}} = \Delta_{\mathbf{k}}$. It is clear that the Hamiltonian is block-diagonal and can be decomposed into two sub-Hamiltonians with $\sigma_z = \pm 1$ characterizing quasi-particles in each block

$$\begin{aligned} \hat{H} = \frac{1}{2}\sum_{\mathbf{k}} \Bigg\{ & \phi_{\uparrow\mathbf{k}}^\dagger \begin{pmatrix} \xi_{\mathbf{k}\uparrow} & \Delta_{\mathbf{k}} \\ \Delta_{\mathbf{k}}^\dagger & -\xi_{-\mathbf{k}\downarrow}^T \end{pmatrix} \phi_{\uparrow\mathbf{k}} \\ & + \phi_{\downarrow\mathbf{k}}^\dagger \begin{pmatrix} \xi_{\mathbf{k}\downarrow} & -\Delta_{\mathbf{k}} \\ -\Delta_{\mathbf{k}}^\dagger & -\xi_{-\mathbf{k}\uparrow}^T \end{pmatrix} \phi_{\downarrow\mathbf{k}} \Bigg\}, \end{aligned} \tag{13}$$

where $\phi_{\uparrow\mathbf{k}} = (\ c_{\mathbf{k}\uparrow}\ \ c_{-\mathbf{k}\downarrow}^\dagger\ )$ and $\phi_{\downarrow\mathbf{k}} = (\ c_{\mathbf{k}\downarrow}\ \ c_{-\mathbf{k}\uparrow}^\dagger\ )$ are quasi-particle operators for spin up and down respectively. Except for a minus sign in the paring amplitude or the pairing matrix $\Delta_{\mathbf{k}}$, Hamiltonians for quasi-particles of both spins are the same. Hence the eigenenergies $E_{\mathbf{k}}$ of quasi-particles are degenerate in spin space (the minus sign can be made to be positive by a rotation in the space of the sub-Hamiltonian with respect to z axis), reflecting the U(1) spin rotation symmetry. Under the particle-hole transformation, $\phi_{\uparrow\mathbf{k}} \to \phi_{\uparrow-\mathbf{k}}^\dagger$, it switches two sub-Hamiltonians. The global superconducting state in Eq.(12) thus has PHS. If $\Delta_{\mathbf{k}}^\dagger \neq \Delta_{\mathbf{k}}$, there is no TRS. However, since S_z is conserved, the classification of the topology is based on each sub-Hamiltonian.[14] The resulting superconducting state is a combination of two sub-systems in class A with TRS, PHS and chiral being absent in each sub-Hamiltonian. Note that each sub-Hamiltonian is characterized by pseudo-spin τ in the charge sector and in general, $\xi_{\mathbf{k}\sigma} \neq \xi_{\mathbf{k}-\sigma}$, there is no PHS symmetry within each sub-Hamiltonian. Since two sub-Hamiltonians are related by the particle-hole transformation, the topological invariants for both spin components are the same. Hence the topological invariant of the whole system is twice of the topological invariant of any subsystem, indicating a $2\mathbb{Z}$ superconductor. The non-trivial topological state will provide Majorana edge modes.

In the following, we will illustrate that there is a QAH state in the superconducting state. Mathematically, we find that in each spin space, there exists a dual transformation that maps the superconducting state into a ferromagnetic insulating state. We consider the $d + id$ superconductivity in the tight-binding model of graphene

$$\begin{aligned} \hat{H}_{\rm SC} = & -t\sum_{\langle i,j\rangle} c_i^\dagger c_j + i\frac{\lambda_{\rm SO}}{3\sqrt{3}} \sum_{\langle\langle i,j\rangle\rangle} \nu_{ij} c_i^\dagger \sigma_z c_j \\ & + \frac{1}{2}\sum_{\langle i,j\rangle} \left[\Delta_{ij} c_i^\dagger (i\sigma_y) \left(c_j^\dagger\right)^T + \text{H.c.} \right] - \mu \sum_i c_i^\dagger c_i. \end{aligned} \tag{14}$$

Here for the $d+id$ pairing, we have $\Delta_{i+\mathbf{d}_l,i} = -\frac{2}{3}\Delta e^{-i\theta_l}$ ($l = 1,2,3$; θ_l increases counterclockwise). After the Fourier transformation, in the basis $c_{\mathrm{SC},\uparrow}(\mathbf{k}) = (\, c_{A\mathbf{k}\uparrow} \;\; c_{B\mathbf{k}\uparrow} \;\; -c^\dagger_{A-\mathbf{k}\downarrow} \;\; c^\dagger_{B-\mathbf{k}\downarrow} \,)^T$, we find that the Bloch Hamiltonian for spin up component is given by

$$\mathcal{H}_{\mathrm{SC},\uparrow}(\mathbf{k}) = \begin{pmatrix} \Lambda_{\mathbf{k}}-\mu & T_{\mathbf{k}} & 0 & \Delta_{\mathbf{k}} \\ T^*_{\mathbf{k}} & -\Lambda_{\mathbf{k}}-\mu & -\Delta_{-\mathbf{k}} & 0 \\ 0 & -\Delta^*_{-\mathbf{k}} & -\Lambda_{\mathbf{k}}+\mu & T_{\mathbf{k}} \\ \Delta^*_{\mathbf{k}} & 0 & T^*_{\mathbf{k}} & \Lambda_{\mathbf{k}}+\mu \end{pmatrix}. \tag{15}$$

Here $T_{\mathbf{k}}$ and $\Lambda_{\mathbf{k}}$ are defined as before. $\Delta_{\mathbf{k}}$ has the same form as $R_{\mathbf{k}}$ except that λ_{R} is replaced by Δ. Comparing Eqs. (15) and (2), we see that the $d+id$ superconductor and the ferromagnetic insulator have equivalent mathematical structure with the following dual transformation:

$d+id$ superconductor		ferromagnetic insulator
Δ	$\leftrightarrow$	λ_{R}
μ	$\leftrightarrow$	M

Clearly, Δ and μ in $d+id$ superconductors are dual to λ_{R} and M in ferromagnetic insulators. However, the mechanism for breaking TRS and PHS is different: TRS is broken by the complex pairing potential in Eq. (15) but it is broken by the exchange potential in Eq. (2) and Δ and M are not dual to each other. In addition, PHS is broken by λ_{SO} in Eq. (15) but it is by λ_{R} in Eq. (2). Note that PHS is broken in each sub-Hamiltonian but it is restored in the superconducting state by including the spin down component.

The existence of the dual transformation implies that the topological invariants for Eqs. (15) and (2) are the same. Therefore, the topological phases with non-vanishing Chern numbers are the same as in Fig. 2(a) by replacing M by μ and λ_{R} by Δ and doubling the Chern numbers, shown in Fig. 2(b). It further implies that these phases with non-vanishing Chern numbers become chiral superconducting phases. Specifically, according to the bulk-edge correspondence for Eq. (2), if the Chern number is C, one gets C edge states at one edge and the other C edge states at the opposite edge in a ribbon. In superconductors, particles (with momentum $\mathbf{k}$) and holes ($-\mathbf{k}$) are mixed, and consequently, a particle-like (positive energy) edge mode will show accompanying with a hole-like (negative energy) mode. Here for class D superconductors, these edge modes are Majorana fermions and thus these particle-like and hole-like modes are not independent but self-charge-conjugate as a Majorana fermion. Hence the Hamiltonian for corresponding edge states can be generally written as

$$\begin{aligned} \hat{H}_{\mathrm{edge}} &= \sum_p \sum_{i=1}^{C} \left(E_p \gamma^\dagger_{p,i}\gamma_{p,i} + \bar{E}_p \bar{\gamma}^\dagger_{-p,i}\bar{\gamma}_{-p,i} \right) \qquad (16) \\ &= \sum_p \sum_{i=1}^{C} \left(E_p \gamma_{-p,i}\gamma_{p,i} - \bar{E}_p \bar{\gamma}_{-p,i}\bar{\gamma}_{p,i} \right), \end{aligned}$$

where $\gamma_{p,i}$ and $\bar{\gamma}_{p,i}$ are the Majorana fermion operators at one and the other edges with corresponding energies being E_p and $\bar{E}_p$, respectively. In above, we only consider positive modes, $E_p, \bar{E}_p \geq 0$. Majorana fermions satisfy $\gamma^\dagger_{p,i} = \gamma_{-p,i}$ and $\{\gamma_{-p,i}, \gamma_{p',j}\} = \delta_{ij}\delta_{pp'}$. C is the Chern number and p is the momentum along the edge. These edge modes are chiral so that $E_{-p} = -E_p$. When there exists, or roughly, in-plane inversion symmetry in the ribbon, we obtain $\bar{E}_p = E_p$ and edge modes at two edges propagating in opposite directions.

For the Hamiltonian $\mathcal{H}_{\mathrm{SC},\uparrow}(\mathbf{k})$, the Chern number of the quasi-HSC phase that corresponds to the SCI/QSH phase also vanishes. For $d+id$ superconductors, this only implies $C_\uparrow = 0$. Since $\mathcal{H}_{\mathrm{SC},\downarrow}(\mathbf{k})$ has the same topology, we find that $C_\downarrow = 0$. Therefore, the spin Chern number C_s, which is $(C_\uparrow - C_\downarrow)/2$, vanishes. However, the quasi-HSC phase does still carry a topological invariant. Analogous to the spin Chern number in a QSH phase, the topological invariant is the pseudo-spin Chern number in the charge space of $\mathcal{H}_{\mathrm{SC},\uparrow}(\mathbf{k})$. If one defines the pseudo-spin quantum number τ such that $c_{A\mathbf{k}\uparrow}$ and $c_{B\mathbf{k}\uparrow}$ have the quantum number $\tau = 1$, while pseudo-spin quantum numbers for $-c^\dagger_{A-\mathbf{k}\downarrow}$ and $c^\dagger_{B-\mathbf{k}\downarrow}$ are $\tau = -1$, the pseudo-spin Chern number

$$C_q = \frac{C_{\tau=1} - C_{\tau=-1}}{2}, \tag{17}$$

where C_τ is the Chern number in the τ sector. C_q is one for both $\mathcal{H}_{\mathrm{SC},\uparrow}(\mathbf{k})$ and $\mathcal{H}_{\mathrm{SC},\downarrow}(\mathbf{k})$, so the quasi-HSC phase in the $d+id$ superconductor is characterized by $C_q = 2$. Since the Chern number vanishes in this phase, we obtain quasi-helical edge states with similar Hamiltonian being given by Eq. (16) with $C = 1$ and both $\gamma_{p,i}$ and $\bar{\gamma}_{p,i}$ describe particle-like quasi-particles at the same edge.

The phase diagram of topology for the $d+id$ superconductor can be also understood from the local pairing symmetry in the momentum space. When the chemical potential μ lies within the gap, λ_{SO}, of normal states, since $\lambda_{\mathrm{SO}} > \Delta$, the system is more like a band insulator than a superconductor and therefore it behaves like a QSH insulator. Note that in reality, superconductivity in an insulator can be induced through proximity effect. As μ is tuned to go beyond the gap and cut the band, the gap of the system is determined by the pairing potential. By expressing the pairing term in the energy basis of electrons in the normal states, we find

$$c_{A\mathbf{k}\uparrow}c_{B-\mathbf{k}\downarrow} \sim \frac{T^*_{\mathbf{k}}}{2\lambda_{\mathrm{SO}}} \left(c_{+,\mathbf{k}\uparrow}c_{+,-\mathbf{k}\downarrow} - c_{-,\mathbf{k}\uparrow}c_{-,\mathbf{k}\downarrow} \right), \tag{18}$$

where $c_\pm$ stand for the upper (lower) energy band near the chemical potential and $T^*_{K/K'+\mathbf{q}} \sim t(q_x \pm i q_y)$ for $q \ll \pi$. Clearly, if the pairing amplitude is $\Delta_{\mathbf{k}}$, the effective pairing symmetry becomes

$$\Delta_{eff}(\mathbf{k}) \sim \Delta_{\mathbf{k}} T^*_{\mathbf{k}}. \tag{19}$$

It is therefore clear that when the pairing function is isotropic s-wave, the effective pairing symmetry is $p \pm ip$-

wave superconductivity locally at Dirac points. However, due to opposite Berry curvatures at K and K', the Chern number vanishes in total for s-wave. For $d+id$ pairing, however, TRS is broken so that local gap functions at K and K' are not equivalent, which results in nontrivial topology. By performing local expansion near Dirac points, we find that $\Delta_{K+\mathbf{q}} \sim \Delta(q_x + iq_y)$, while $\Delta_{K'+\mathbf{q}} \sim \Delta$. Therefore, local Berry curvatures at K and K' do not get canceled and both $c_\pm$ bands get nonvanishing finite Chern numbers.

Finally, we note in passing that while in the above dual transformation, only NN pairing and the Rashba SOC are considered, the duality is valid when NNN couplings are included. Specifically, for the NNN pairing on the same sub-lattice, there is also a corresponding dual SOC term in the ferromagnetic insulating system. For $d+id$-wave superconductors, we find that the dual term to the NNN pairing order parameter is the NNN Rashba spin-orbit interaction that is shown to exist in silicene due to the buckled structure.[38,39]

C. Class D superconductor with ferromagnetism

We now combine both ferromagnetic and superconducting models in Eqs. (1) and (14). This would be the model to describe the situation that occurs when a $d+id$ superconductor is placed in proximity to a ferromagnet so that the exchange field is induced in the $d+id$ superconducting state. In this case, both the Rashba spin-orbit interaction and the pairing potential are present, hence S_z is no longer conserved. The system belongs to the class D superconductor.[14]

If we adopt the basis for the electron, $\psi = \begin{pmatrix} c_{\rm FM}(\mathbf{k}) \\ c^\dagger_{\rm FM}(-\mathbf{k}) \end{pmatrix}$ where $c_{\rm FM}(\mathbf{k})$ is the same basis used in Eq. (2), the Bloch Hamiltonian is given by

$$\mathcal{H}_{\rm SC/FM}(\mathbf{k}) = \begin{pmatrix} \mathcal{H}_{\rm FM}(\mathbf{k}) - \mu\mathbb{I} & \mathcal{D}(\mathbf{k}) \\ \mathcal{D}^\dagger(\mathbf{k}) & -\mathcal{H}^T_{\rm FM}(-\mathbf{k}) + \mu\mathbb{I} \end{pmatrix}, \tag{20}$$

where $\mathcal{H}_{\rm FM}(\mathbf{k})$ is given by Eq. (2) and $\mathcal{D}(\mathbf{k})$ is the pairing matrix given by

$$\mathcal{D}(\mathbf{k}) = \begin{pmatrix} 0 & 0 & 0 & -\Delta_{\mathbf{k}} \\ 0 & 0 & -\Delta_{-\mathbf{k}} & 0 \\ 0 & \Delta_{\mathbf{k}} & 0 & 0 \\ \Delta_{-\mathbf{k}} & 0 & 0 & 0 \end{pmatrix}. \tag{21}$$

Note that the Hamiltonian can not be decomposed into two sub-Hamiltonians due to nonconserving S_z. In addition, although the Rashba SOC breaks inversion symmetry, in the proximity effect, neglecting the triplet pairing is an acceptable approximation.

The Hamiltonian $\mathcal{H}_{\rm SC/FM}(\mathbf{k})$ is self-dual. This can be seen by constructing a unitary transformation U that brings ψ into the form $\begin{pmatrix} c_{\rm SC}(\mathbf{k}) \\ c^\dagger_{\rm SC}(-\mathbf{k}) \end{pmatrix}$. Let $\begin{pmatrix} c_{\rm SC}(\mathbf{k}) \\ c^\dagger_{\rm SC}(-\mathbf{k}) \end{pmatrix} = U\psi$, we find that U is given by

$$U = \begin{pmatrix} 1 & 0 & 0 & 0 \\ 0 & 0 & 0 & -\sigma_z \\ 0 & 1 & 0 & 0 \\ 0 & 0 & -\sigma_z & 0 \end{pmatrix}, \tag{22}$$

where 1 and σ_z are 2×2 matrices. As a consequence of duality, one finds

$$U\mathcal{H}_{\rm SC/FM}(M,\mu,\lambda_{\rm R},\Delta)U^\dagger = \mathcal{H}_{\rm SC/FM}(\mu,M,\Delta,\lambda_{\rm R}). \tag{23}$$

Therefore, the topology of electronic structures for $d+id$ superconductors in proximity to ferromagnets is symmetric between (M, μ) and ($\lambda_{\rm R}$, Δ). This implies that investigating weak superconductivity ($\Delta < \lambda_{\rm R}$) and weak ferromagnetism ($M < \mu$) allows one to access topological phases of strong superconductivity and strong ferromagnetism. In reality, since it is not easy to change Δ and M, the duality allows one to tune $\lambda_{\rm R}$ and μ to access different topological phases of the system.

Typical topological phase diagrams for $\mathcal{H}_{\rm SC/FM}$ are shown in Fig. 4. Here Figure 4 (a) shows different chiral superconducting phases for a pure $d+id$ superconductor with $M=0$. It is seen that for small gap amplitude (weak coupling limit), $d+id$-wave superconductors are always in chiral superconducting phases with Chern number being ± 2. Figure 4 (b) shows chiral superconducting phases for a $d+id$ superconductor mixed with moderate ferromagnetism. The largest Chern number can go up to 4. In Fig. 4 (c), we show the topological phase diagram for weak superconductivity in $\mu - M$ space at ($t/\lambda_{\rm SO}$, $\lambda_{\rm R}/\lambda_{\rm SO}$, $\Delta/\lambda_{\rm SO}$) = (10, 0.4, 0.1). The Chern number can be 0, -2, ± 4, and 6 with 6 being the largest possible Chern number in this system. The zero Chern number at the center of the phase diagram is the quantum pseudo-spin Hall phase in the charge sector with $C_q = 2$. As indicated before, the phase boundaries are the band touching loci and the change of Chern number across the boundaries is the change of total angular momenta of the filled bands. Because the exchange of angular momentum happens simultaneously at K and K', the Chern number must be even.

Figure 5 illustrates the bulk-edge correspondence for the phase diagram shown in Fig. 4 (c). Here the spectra of a zigzag ribbon in different topological phases are computed to check the consistency of equality of the bulk Chern number and the number of chiral edge modes. Here in the presence of in-plane inversion symmetry for each chiral edge mode at one edge with energy and momentum (E,p), there is another mode at the other side with $(E,-p)$, and they are Majorana fermions, in agreement with Eq. (16).

We now illustrate the physical mechanism for the behavior of phase diagram in Fig. 4(c) in the weak coupling limit. In this limit, the pairing is weak and hence considering pairing between intraband electrons is sufficient. A

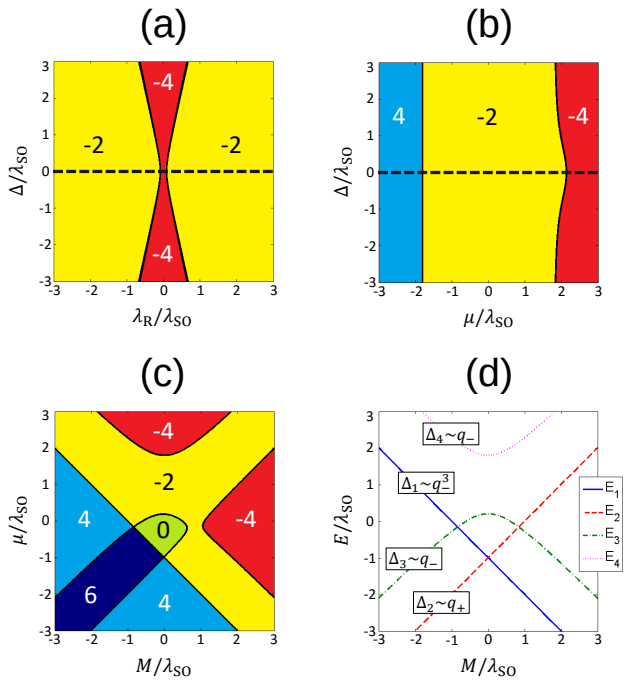

FIG. 4. (Color online) Typical topological phase diagrams for a $d + id$ superconductor in proximity to a ferromagnet. Numbers shown in colored areas are the corresponding Chern numbers. (a) Δ versus the Rashba spin-orbit coupling λ_R at $\mu/\lambda_{SO} = 1.2$ and $M = 0$. (b) Δ versus μ for $\lambda_R/\lambda_{SO} = 0.4$ and $M/\lambda_{SO} = 0.8$. (c) Phase diagram of weak superconductivity ($\Delta/\lambda_{SO} = 0.1$) for μ versus M. Here $t/\lambda_{SO} = 10$ and $\lambda_R/\lambda_{SO} = 0.4$. (d) Eigenenergies at the K point for four normal-state bands ($\Delta = 0$) as functions of M. Here $\lambda_R/\lambda_{SO} = 0.4$. Tagged boxes display gap functions near K for corresponding bands (see text).

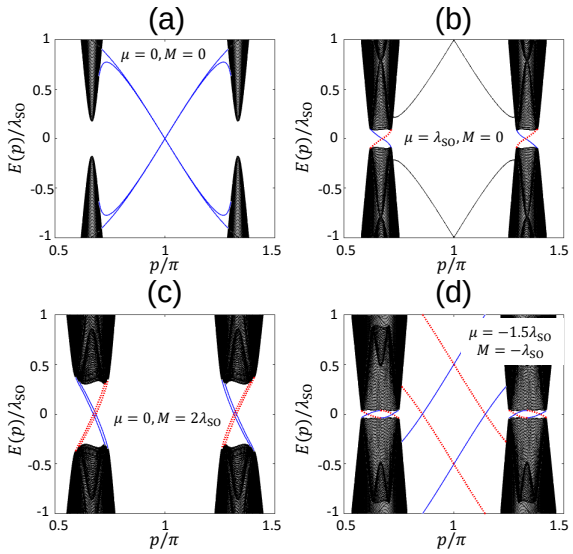

FIG. 5. (Color online) Bulk-edge correspondence for zigzag ribbons in different topological superconducting phases. (a) $C = 0$, $C_q = 2$, (b) $C = -2$ (c) $C = -4$, and (d) $C = +6$, respectively. Here red and blue lines denote edge states at opposite edges. The common parameters are $(t/\lambda_{SO}, \lambda_R/\lambda_{SO}, \Delta/\lambda_{SO}) = (10, 0.4, 0.1)$. The number of lattice points for width of the ribbons is 800.

superconducting state can be generally described by

$$\mathcal{H}(q) = \begin{pmatrix} \xi_q & \Delta_q \\ \Delta_q^* & -\xi_{-q} \end{pmatrix}. \tag{24}$$

Here q is the momentum relative to K or K' point, ξ_q is the kinetic energy relative to the chemical potential, and Δ_q is the pairing gap function. For a nontrivial superconducting state, the chemical potential is within an energy band so that ξ_q must change sign in the Brillouin zone. Furthermore, the gap function is generally a representation of a rotational group and can be generally expressed as $\Delta_q = \Delta q_\pm^n$ with $q_\pm = q_x \pm i q_y$ and $n \in \mathbb{N}$. As an example, the case of $n = 1$ is the well-known $p \pm ip$ CSC. Under a rotation by ϕ, the gap function is an eigenfunction to the rotation, $q_\pm^n \to e^{\mp in\phi} q_\pm^n$. Hence the gap function is generally a representation of rotational group. In other words, the gap function carries angular momentum. Now from Eqs. (9) and (10), for three-fold rotation $\phi = 2\pi/3$, the rotation eigenvalues of a Cooper pair for energy bands 1, 2, 3, and 4 are $e^{i4\pi/3}$, $e^{-i4\pi/3}$, 1, and 1, respectively. On the other hand, the $d + id$ pairing carries an extra angular momentum $l = -1$ ($\eta = e^{i2\pi/3}$) such that the gap functions of bands have rotation eigenvalues $e^{i6\pi/3}$, $e^{-i2\pi/3}$, $e^{i2\pi/3}$, and $e^{i2\pi/3}$, respectively. As a result, the gap functions behave as $\Delta_1 \sim q_-^3$, $\Delta_2 \sim q_+$, $\Delta_3 \sim q_-$, and $\Delta_4 \sim q_-$. Detailed derivations for the rotation symmetry in superconducting states are referred to Appendix B.

In Fig. 4(d), we show eigenenergies of four bands $E_{1,2,3,4}$ and their corresponding gap functions $\Delta_{1,2,3,4}$. Comparing Figs. 4(c) and (d), the close similarity between the phase boundaries and eigenenergies are found with a small discrepancy that might result from finite $\Delta/\lambda_{SO} = 0.1$. Since the eigenenergies at K (or K') are the top or the bottom of the associated energy bands, when the chemical potential passes across these energies, it can be either falling within an energy band or outside an energy band, depending on the direction of the chemical potential moves. Clearly, this indicates a topological phase transition and hence a change in the Chern number. The value of the changed Chern number is determined by the gap functions and the direction of chemical potential enters/leaves a band. By including both contributions from K and K', the topological phase transitions in Fig. 4(c) are reproduced by using Fig. 4(d). We refer readers to Appendix C for more detailed explanations.

III. DISCUSSION AND SUMMARY

In summary, we have demonstrated a dual transformation between a $d+id$ superconductor and a ferromagnetic insulator in a honeycomb lattice with the former being a CSC and the latter being a QAH insulator. The $d+id$ superconductor can be viewed as a combination of two QAH insulators, which map into one another under particle-hole transformation, and thus carries a $2\mathbb{Z}$ topological invariant. When the superconducting pairing amplitude is weak and the chemical potential falls within the SOC gap, the superconductor is quasi-helical and its dual phase is the SCI state with a small Rashba SOC and weak ferromagnetism. Moreover, when both superconductivity and ferromagnetism are included, the system in class D possesses self-duality: $\mu \leftrightarrow M$ and $\Delta \leftrightarrow \lambda_{\rm R}$. This implies that topological effects of strong superconductivity or ferromagnetism can be observed in topological states with weak superconductivity or ferromagnetism.

We have also explored the topological superconductor from the effective low-energy Hamiltonian, Eq. (24), in which the topology is encoded in the gap function Δ_q when the normal-state Fermi surface is present. The nontrivial topology is present when the gap function $\Delta_q = \Delta q_+^{n_+} q_-^{n_-}$ with $n_+ - n_- \neq 0$, which can be determined by the rotational eigenvalues: $\Delta_{\mathfrak{R}\mathbf{q}} = \eta^K \eta^{K'} e^{i\phi} \Delta_{\mathbf{q}}$, where $\eta^{K/K'}$ is the phase gained under rotation from the band electron at K/K' and $e^{i\phi}$ from the $d+id$-wave nature. Equivalently, the criterion for non-trivial topology is to require $\eta^K \eta^{K'} e^{i\phi} \neq 1$. From this inequality, it is clear that the time-reversal invariant would demand $\eta^K = (\eta^{K'})^*$ and $e^{i\phi} = 1$, hence for a nontrivial two-dimensional superconductor with non-vanishing Chern number, breaking TRS is essential. The inequality also explains that why an s-wave ($e^{i\phi} = 1$) superconductor can be topologically nontrivial if TRS is broken to in normal states such that $\eta^K \neq (\eta^{K'})^*$.

Finally, we discuss experimental features that can be observed for topological superconductors. According to the bulk-edge correspondence, the Chern number for topological superconductors is the number of Majorana edge modes. Since these midgap modes are localized at edges, they will play important roles at low voltage of the tunneling conductance.[25,40] For the Hall conductivity measurements, it is known that the Hall conductivity will be quantized in an insulator as $\sigma_{\rm H} = Ce^2/h$, C the Chern number,[1] and deviate from the quantized value when doped into a metal. In superconductors, because charges are not conserved,the Hall conductivity is no longer quantized even if the Chern number is nonvanishing. In the weak pairing limit, the change in the Hall conductivity comes from the change in the occupation number and the change of Berry curvature,[41] and thus the Hall conductivity decreases against the superconducting gap. Although the Hall conductivity does not show a clear signature to differentiate a topological superconductor from a trivial one, its derivatives deliver the signature of topological phase transitions.[42]

On the other hand, due to the energy conservation, the topological invariant, Chern numbers, can still be revealed in the thermal Hall conductivity. It is known that the thermal Hall conductivity of the topological superconductors in the low temperature limit is given by $\kappa_{xy} = \frac{C}{2}\frac{\pi T}{6}$ with the coefficient to the temperature T being quantized.[43–45] Here the appearance of half the Chern number is a reflection of the half-fermion nature for Majorana modes. Different topological phases shown in Fig. 4(c) can be thus identified by measuring the thermal Hall conductivity.

ACKNOWLEDGMENTS

This work was supported by Ministry of Science and Technology (MoST), Taiwan. SMH would like to thank Hsin Lin for his helpful suggestions and also appreciate NCTS for accommodation support. We also acknowledge support by Academia Sinica Research Program on Nanoscience and Nanotechnology, Taiwan.

Appendix A: Rotation symmetry for non-superconducting states

In this Appendix, we examine the rotation symmetry in the non-superconducting states and will find the rotation eigenvalues of four bands at K and K' valleys for non-superconducting states. In the honeycomb lattice, there exists three-fold rotation symmetry, satisfying $\left[\hat{R}, \hat{H}\right] = 0$, where $\hat{R}$ stands for a clockwise three-fold rotation. For the Bloch Hamiltonian, it reads

$$\mathcal{R}\mathcal{H}(\mathbf{k})\mathcal{R}^\dagger = \mathcal{H}(\mathfrak{R}\mathbf{k}), \tag{A1}$$

where $\mathfrak{R}\mathbf{k}$ is the transformed wave vector $\mathbf{k}$ under rotation and $\mathcal{R}$ is the rotation matrix for a given representation, resulting from $\hat{R}\psi^\dagger_{\mathbf{k}}\hat{R}^{-1} = \psi^\dagger_{\mathfrak{R}\mathbf{k}}\mathcal{R}$. Since K and K' are rotation-invariant momenta, which satisfy $\mathfrak{R}K = K - \mathbf{G}_2$ and $\mathfrak{R}K' = K' + \mathbf{G}_2$ with reciprocal lattice $\mathbf{G}_2 = 2\pi(1, 1/\sqrt{3})$, the energy eigenstates are thus also the rotation eigenstates. After rotation, the basis will transform as $c^\dagger_{AK\sigma} \rightarrow c^\dagger_{A(K-\mathbf{G}_2)\sigma} e^{i\sigma\pi/3} = c^\dagger_{AK\sigma} e^{i\sigma\pi/3}$ and $c^\dagger_{BK\sigma} \rightarrow c^\dagger_{B(K-\mathbf{G}_2)\sigma} e^{i\sigma\pi/3} = c^\dagger_{BK\sigma} e^{i\sigma\pi/3} e^{-i2\pi/3}$, where $e^{-i2\pi/3} = e^{i(-\mathbf{G}_2)\cdot(-\mathbf{d}_1)}$ comes from the non-primitive sub-lattice vector in the unit cell. By expanding the Hamiltonian around K and K' with $\mathbf{q}$ being the deviation of momentum, we find

$$\mathcal{R}\mathcal{V}_G\mathcal{H}^K(\mathbf{q})\mathcal{V}_G^\dagger\mathcal{R}^\dagger = \mathcal{H}^K(\mathfrak{R}\mathbf{q}), \tag{A2}$$

$$\mathcal{R}\mathcal{V}_G^\dagger\mathcal{H}^{K'}(\mathbf{q})\mathcal{V}_G\mathcal{R}^\dagger = \mathcal{H}^{K'}(\mathfrak{R}\mathbf{q}), \tag{A3}$$

where $\mathcal{R} = \exp(i\sigma_z\pi/3)$ and $\mathcal{V}_G = \exp[i(\tau_z - 1)\pi/3]$ for σ_z on spin and τ_z on sub-lattice space. The rotation

eigenvalues of states at K and K' are the eigenvalues of $\mathcal{R}\mathcal{V}_G$ and $\mathcal{R}\mathcal{V}_G^\dagger$, respectively.

To find the eigenstates, we need the expansion of functions for the momentum around K, K' with small deviation $\mathbf{q}$, $T_{K/K'+\mathbf{q}} \approx \pm\frac{\sqrt{3}}{2}tq_\mp$, $\Lambda_{K/K'+\mathbf{q}} \approx \mp\lambda_{\rm SO}$, $R_{K+\mathbf{q}} \approx -\frac{i}{\sqrt{3}}\lambda_{\rm R}q_+$ and $R_{K'+\mathbf{q}} \approx -i2\lambda_{\rm R}$ with $q_\pm = q_x \pm iq_y$. The Bloch Hamiltonian at K, Eq. (2), is

$$\mathcal{H}_{\rm FM}^K = \begin{pmatrix} -\lambda_{\rm SO}-M & 0 & 0 & 0 \\ 0 & \lambda_{\rm SO}-M & i2\lambda_{\rm R} & 0 \\ 0 & -i2\lambda_{\rm R} & \lambda_{\rm SO}+M & 0 \\ 0 & 0 & 0 & -\lambda_{\rm SO}+M \end{pmatrix}, \tag{A4}$$

whose eigenstates are given by

$$\begin{aligned} |\gamma_1\rangle_K &= \begin{pmatrix} 1, & 0, & 0, & 0 \end{pmatrix}^T, \\ |\gamma_2\rangle_K &= \begin{pmatrix} 0, & 0, & 0, & 1 \end{pmatrix}^T, \\ |\gamma_3\rangle_K &= \begin{pmatrix} 0, & -i\sin\frac{\theta}{2}, & \cos\frac{\theta}{2}, & 0 \end{pmatrix}^T, \\ |\gamma_4\rangle_K &= \begin{pmatrix} 0, & \cos\frac{\theta}{2}, & -i\sin\frac{\theta}{2}, & 0 \end{pmatrix}^T, \end{aligned} \tag{A5}$$

with the corresponding eigenenergies being

$$\begin{aligned} E_1 &= -\lambda_{\rm SO}-M, \\ E_2 &= -\lambda_{\rm SO}+M, \\ E_3 &= \lambda_{\rm SO}-\sqrt{M^2+4\lambda_{\rm R}^2}, \\ E_4 &= \lambda_{\rm SO}+\sqrt{M^2+4\lambda_{\rm R}^2}, \end{aligned} \tag{A6}$$

respectively. Here $\theta = -\arctan\frac{2\lambda_{\rm R}}{M}$. The rotation eigenvalues of these four states are obtained by applying $\mathcal{R}\mathcal{V}_G$. We obtain

$$\begin{aligned} \eta_1^K &= e^{i\pi/3}, \\ \eta_2^K &= e^{-i3\pi/3}, \\ \eta_3^K &= e^{-i\pi/3}, \\ \eta_4^K &= e^{-i\pi/3}. \end{aligned} \tag{A7}$$

For the case of $M > 0$, the band inversion happens between the the second $|\gamma_2\rangle$ and the third band $|\gamma_3\rangle$ and hence the rotation eigenvalue changes by $e^{i2\pi/3}$.

On the other hand, for the K' point, the Hamiltonian is

$$\mathcal{H}_{\rm FM}^{K'} = \begin{pmatrix} \lambda_{\rm SO}-M & 0 & 0 & -i2\lambda_{\rm R} \\ 0 & -\lambda_{\rm SO}-M & 0 & 0 \\ 0 & 0 & -\lambda_{\rm SO}+M & 0 \\ i2\lambda_{\rm R} & 0 & 0 & \lambda_{\rm SO}+M \end{pmatrix}, \tag{A8}$$

and the eigenstates are given by

$$\begin{aligned} |\gamma_1\rangle_{K'} &= \begin{pmatrix} 0, & 1, & 0, & 0 \end{pmatrix}^T, \\ |\gamma_2\rangle_{K'} &= \begin{pmatrix} 0, & 0, & 1, & 0 \end{pmatrix}^T, \\ |\gamma_3\rangle_{K'} &= \begin{pmatrix} \cos\frac{\theta}{2}, & 0, & 0, & i\sin\frac{\theta}{2} \end{pmatrix}^T, \\ |\gamma_4\rangle_{K'} &= \begin{pmatrix} i\sin\frac{\theta}{2}, & 0, & 0, & \cos\frac{\theta}{2} \end{pmatrix}^T. \end{aligned} \tag{A9}$$

Here the eigenenergies are the same as those given by Eqs.(A6). From the eigenstates, their rotation eigenvalues of $\mathcal{R}\mathcal{V}_G^\dagger$ are

$$\begin{aligned} \eta_1^{K'} &= e^{i3\pi/3}, \\ \eta_2^{K'} &= e^{-i\pi/3}, \\ \eta_3^{K'} &= e^{i\pi/3}, \\ \eta_4^{K'} &= e^{i\pi/3}, \end{aligned} \tag{A10}$$

For $M > 0$, the band inversion between $|\gamma_2\rangle$ and $|\gamma_3\rangle$ at K' also coincides with the change of rotation eigenvalue by $e^{i2\pi/3}$.

Appendix B: Rotation symmetry in the superconducting states

In this Appendix, we elucidate the rotation symmetry in superconducting state. We have demonstrated that there is a three-fold rotation symmetry in the non-superconducting state with the consequence $\left[\hat{R}, \hat{H}\right] = 0$ in Appendix A. In unconventional superconductors, the pairing term is not rotation-invariant but it forms a representation of the rotational group by obeying $\hat{\Delta} \to e^{i\phi}\hat{\Delta}$ under a three-fold rotation. Here for the $d+id$-wave in our case, $\phi = 2\pi/3$. The extra phase ϕ results from the internal angular momentum of the Cooper pair and can be combined with the U(1) phase associated with the spontaneous U(1) gauge symmetry breaking in the superconducting state. As a result, the rotation symmetry is not really broken and can be restored by a gauge transformation.

In order to include phases associated with angular momenta of Cooper pairs, the condition for the rotational symmetry, Eq. (A1), needs to be modified. If we adopt the same rotation matrix $\mathcal{R}$ for both particle and hole, a BdG Hamiltonian, $\mathcal{H}_{\rm SC}(\mathbf{k})$, is rotation-invariant if it satisfies

$$\bar{\mathcal{R}}\bar{\mathcal{V}}\mathcal{H}_{\rm SC}(\mathbf{k})\bar{\mathcal{V}}^\dagger\bar{\mathcal{R}}^\dagger = \mathcal{H}_{\rm SC}(\mathfrak{R}\mathbf{k}), \tag{B1}$$

where $\bar{\mathcal{R}} = {\rm diag}(\ \mathcal{R},\ \mathcal{R}^*\ )$ and $\bar{\mathcal{V}} = {\rm diag}(\ 1,\ e^{-i\phi}\ )$ with the first elements ($\mathcal{R}$ and 1) and the second elements ($\mathcal{R}^*$ and $e^{-i\phi}$) acting on particle and hole space, respectively. The matrix $\bar{V}$ reproduces the phase ϕ for superconductors under the operation of rotation.

We now derive the effective pairing symmetries for bands around K and K'. We shall start from the low-energy Hamiltonian for a given band around K or K' by

$$\mathcal{H}_{\rm SC}^{K/K'}(\mathbf{q}) = \begin{pmatrix} \xi_{\mathbf{q}} & \Delta_{\mathbf{q}} \\ \Delta_{\mathbf{q}}^* & -\xi_{-\mathbf{q}} \end{pmatrix}. \tag{B2}$$

Here in the weak-coupling limit, only intra-band pairing is considered and $\Delta_{\mathbf{q}}$ is non-vanishing only in a small

energy range around the chemical potential. Similar to Eqs. (A2) and (A3), the rotation symmetry requires

$$\bar{\mathcal{R}}\bar{\mathcal{V}}\mathcal{H}_{\rm SC}^{K/K'}(\mathbf{q})\bar{\mathcal{V}}^{\dagger}\bar{\mathcal{R}}^{\dagger}=\mathcal{H}_{\rm SC}^{K/K'}(\mathfrak{R}\mathbf{q}). \tag{B3}$$

For each band, $\mathcal{R}$ is replaced by the corresponding rotation eigenvalues $\eta^{K/K'}$ that are obtained for the non-superconducting state in Eqs. (A7) and (A10) and we obtain

$$\Delta_{\mathfrak{R}\mathbf{q}}=\eta^{K}\eta^{K'}e^{i\phi}\Delta_{\mathbf{q}}. \tag{B4}$$

The phase in Eq. (B4) results from the rotation of a Cooper pair and consists of phases from their composite electrons at K and K' and the nontrivial phase from the symmetry of the gap function. For the $d+id$-wave with $e^{i\phi}=e^{i2\pi/3}$, the gap function can be considered to carry angular momentum $l=-1$. In general, the pairing potential near K and K' can be expressed as $\Delta_{\mathbf{q}}=\Delta q_{+}^{n_{+}}q_{-}^{n_{-}}$ with $q_{\pm}=q_x\pm iq_y$ and $n_{\pm}\in\mathbb{N}$. By using Eq. (B4) and the identity, $\mathfrak{R}q_{\pm}=e^{\mp i2\pi/3}q_{\pm}$, we find that the total phase associated with $\Delta_{\mathbf{q}}$ is $\eta^{K}\eta^{K'}e^{i\frac{2\pi}{3}}=e^{i\frac{2\pi}{3}(n_{-}-n_{+})}$ with $n_{\pm}$ being determined by η^{K} and $\eta^{K'}$ of the corresponding band. Using η^{K} and $\eta^{K'}$ in Eqs. (A7) and (A10), we conclude that the effective gap functions for four bands behave as

$$\begin{aligned}&\Delta_1\sim q_{-}^{3},\\&\Delta_2\sim q_{+},\\&\Delta_3\sim q_{-},\\&\Delta_4\sim q_{-}.\end{aligned} \tag{B5}$$

Appendix C: Chern Number in the weak coupling limit

In this Appendix, we present a simple way to understand the topological number of a superconductor in the weak coupling limit. Here in weak coupling limit, one assumes that the pairing is weak and only pairing between intra-band electrons is considered. In the weak coupling, the superconducting gap function on the Fermi surface of a given band is sufficient to determine the Chern number of superconductivity.

First of all, we choose the convention for the Berry connection as

$$\mathbf{A}_n(\mathbf{k})=i\left\langle u_n(\mathbf{k})\right|\left|\nabla_{\mathbf{k}}\right|u_n(\mathbf{k})\rangle, \tag{C1}$$

where u_n is the Bloch wavefunction of band n. In this convention, the Chern number is the integral of Berry curvature $\nabla_{\mathbf{k}}\times\mathbf{A}_n(\mathbf{k})$ from the filled bands over the Brillouin zone and can be formulated as

$$C=-\int_{\rm BZ}\frac{d^2k}{2\pi}\sum_{\alpha,\beta} \tag{C2}$$
$$2{\rm Im}\left\{\frac{\langle u_\alpha(\mathbf{k})\left|v_x(\mathbf{k})\right|u_\beta(\mathbf{k})\rangle\langle u_\beta(\mathbf{k})\left|v_y(\mathbf{k})\right|u_\alpha(\mathbf{k})\rangle}{\left[E_\alpha(\mathbf{k})-E_\beta(\mathbf{k})\right]^2}\right\},$$

where α (β) denotes filled (unfilled) bands and $v_i(\mathbf{k})=\frac{\partial H(\mathbf{k})}{\partial k_i}$ ($i=x,\,y$).

Let us start a Hamiltonian in the form

$$\mathcal{H}(q)=\begin{pmatrix}\xi_q & \Delta q_{+}^{n_{+}}q_{-}^{n_{-}}\\ \Delta^{*}q_{-}^{n_{+}}q_{+}^{n_{-}} & -\xi_q\end{pmatrix}, \tag{C3}$$

with $q_{\pm}=q_x\pm iq_y$ and $n_{\pm}\in\mathbb{N}$. The Hamiltonian describes a superconductor, in which ξ_q is the kinetic energy with respect to the chemical potential and $\Delta q_{+}^{n_{+}}q_{-}^{n_{-}}$ is the gap function. By using the Pauli matrices σ, the Hamiltonian can be rewritten as

$$\mathcal{H}(q)=E(q)\mathbf{h}_q\cdot\sigma \tag{C4}$$

with $E(q)=\sqrt{\xi_q^2+|\Delta|\,q^{2(n_{+}+n_{-})}}$. Here $\mathbf{h}_q=(\sin\Theta_q\cos\Phi_q,\sin\Theta_q\sin\Phi_q,\cos\Theta_q)$ is the unit vector with Θ_q and Φ_q characterizing its direction. The Chern number can be then expressed as

$$\begin{aligned}C&=\frac{1}{4\pi}\int d^2q\mathbf{h}_q\cdot\frac{\partial\mathbf{h}_q}{\partial q_x}\times\frac{\partial\mathbf{h}_q}{\partial q_y}\\&=\frac{1}{4\pi}\int d^2q\epsilon_{ij}\partial_{q_i}\cos\Theta_q\partial_{q_j}\Phi_q.\end{aligned} \tag{C5}$$

Eq.(C4) indicates that the Hamiltonian can be viewed as a mapping from R^2 in q space to S^2 in (Θ,Φ) and $\epsilon_{ij}\partial_{q_i}\cos\Theta_q\partial_{q_j}\Phi_q$ is the Jacobian between them such that the Chern number stands for the covering times of the fields (Θ,Φ) over a sphere. Therefore, if ξ can change sign with q, namely $\xi_{q=0}\xi_{q\sim\pi}<0$, the chemical potential is within the energy band and the Chern number is found to be (when the weak coupling condition, $\Delta_{q\sim\pi}=0$, is applied implicitly)

$$C={\rm sgn}(\xi_{q=0})\left(n_{-}-n_{+}\right). \tag{C6}$$

On the other hand, if ξ does not change sign with q, the Chern number is found to be zero. In other words, the Hamiltonian in Eq. (C3) describes a nontrivial superconductor if the chemical potential passes through the band (ξ_q will change sign), otherwise, it is a trivial superconductor. For a nontrivial superconductor, the normal-state Fermi surface is hole-like if $\xi_{q=0}>0$ and electron-like if $\xi_{q=0}<0$. In Fig. 6, we illustrates how the Chern number changes when the chemical potential moves out of the band .

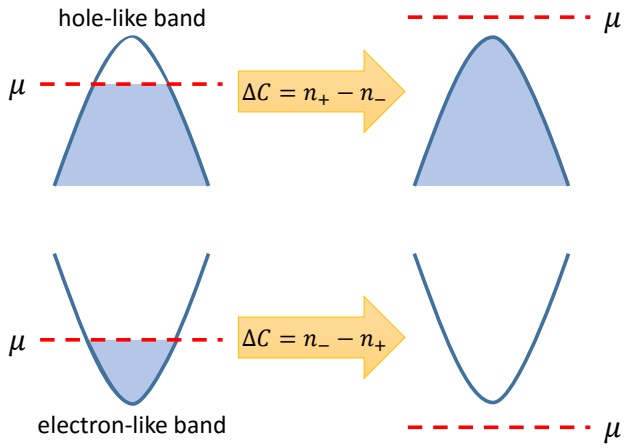

FIG. 6. (Color online) Change of the Chern number ΔC of a superconducting state with a (local) gap function $\Delta q_+^{n_+} q_-^{n_-}$ [refer to Eq. (C3)]. Here $n_\pm \in \mathbb{N}$. A nontrivial superconducting state emerges when the chemical potential μ cuts through the band of the normal state. Upper panel: Change of the Chern number when the normal state goes from hole-like band to be a completely filled band. Lower panel: Change of the Chern number when the normal state goes from electron-like band to be a unfilled band. Note that the Chern number is not affected by the sign of the pairing amplitude Δ.

[1] D. J. Thouless, M. Kohmoto, M. P. Nightingale, and M. den Nijs, Phys. Rev. Lett. **49**, 405 (1982).
[2] B. I. Halperin, Phys. Rev. B **25**, 2185 (1982).
[3] Y. Hatsugai, Phys. Rev. Lett. **71**, 3697 (1993).
[4] C.-Z. Chang, J. Zhang, X. Feng, J. Shen, Z. Zhang, M. Guo, K. Li, Y. Ou, P. Wei, L.-L. Wang, Z.-Q. Ji, Y. Feng, S. Ji, X. Chen, J. Jia, X. Dai, Z. Fang, S.-C. Zhang, K. He, Y. Wang, L. Lu, X.-C. Ma, and Q.-K. Xue, Science **340**, 167 (2013).
[5] S.-M. Huang, S.-T. Lee, and C.-Y. Mou, Phys. Rev. B **89**, 195444 (2014).
[6] C. L. Kane and E. J. Mele, Phys. Rev. Lett. **95**, 146802 (2005).
[7] C. L. Kane and E. J. Mele, Phys. Rev. Lett. **95**, 226801 (2005).
[8] B. A. Bernevig, T. L. Hughes, and S.-C. Zhang, Science **314**, 1757 (2006).
[9] M. König, S. Wiedmann, C. Brüne, A. Roth, H. Buhmann, L. W. Molenkamp, X.-L. Qi, and S.-C. Zhang, Science **318**, 766 (2007).
[10] A. Roth, C. Brüne, H. Buhmann, L. W. Molenkamp, J. Maciejko, X.-L. Qi, and S.-C. Zhang, Science **325**, 294 (2009).
[11] H. Zhang, C.-X. Liu, X.-L. Qi, X. Dai, Z. Fang, and S.-C. Zhang, Nature physics **5**, 438 (2009).
[12] M. R. Zirnbauer, J. Math. Phys. **37**, 4986 (1996).
[13] A. Altland and M. R. Zirnbauer, Phys. Rev. B **55**, 1142 (1997).
[14] A. P. Schnyder, S. Ryu, A. Furusaki, and A. W. W. Ludwig, Phys. Rev. B **78**, 195125 (2008).
[15] A. Kitaev, AIP Conf. Proc. **1134**, 22 (2009).
[16] C.-K. Chiu, J. C. Y. Teo, A. P. Schnyder, and S. Ryu, ArXiv e-prints (2015), arXiv:1505.03535 [cond-mat.mes-hall].
[17] D. M. Lee, Rev. Mod. Phys. **69**, 645 (1997).
[18] H. Tou, Y. Kitaoka, K. Asayama, N. Kimura, Y. Ōnuki, E. Yamamoto, and K. Maezawa, Phys. Rev. Lett. **77**, 1374 (1996).
[19] I. Eremin, D. Manske, S. Ovchinnikov, and J. Annett, Annalen der Physik **13**, 149 (2004).
[20] Y. Maeno, S. Kittaka, T. Nomura, S. Yonezawa, and K. Ishida, Journal of the Physical Society of Japan **81**, 011009 (2012).
[21] L. Fu and C. L. Kane, Phys. Rev. Lett. **100**, 096407 (2008).
[22] V. Mourik, K. Zuo, S. M. Frolov, S. R. Plissard, E. P. A. M. Bakkers, and L. P. Kouwenhoven, Science **336**, 1003 (2012).
[23] Y. Oreg, G. Refael, and F. von Oppen, Phys. Rev. Lett. **105**, 177002 (2010).
[24] F. Zhang, C. L. Kane, and E. J. Mele, Phys. Rev. Lett. **111**, 056402 (2013).
[25] J.-T. Kao, S.-M. Huang, C.-Y. Mou, and C. C. Tsuei, Phys. Rev. B **91**, 134501 (2015).
[26] R. B. Laughlin, Phys. Rev. Lett. **80**, 5188 (1998).
[27] J. E. Moore and D.-H. Lee, Phys. Rev. B **69**, 104511 (2004).
[28] B. Rosenstein, I. Shapiro, and B. Shapiro, Journal of Low Temperature Physics **173**, 289 (2013).

[29] W.-C. Lee, S.-C. Zhang, and C. Wu, Phys. Rev. Lett. **102**, 217002 (2009).
[30] A. M. Black-Schaffer, Phys. Rev. Lett. **109**, 197001 (2012).
[31] M. Sato, Y. Takahashi, and S. Fujimoto, Phys. Rev. Lett. **103**, 020401 (2009).
[32] D. N. Sheng, Z. Y. Weng, L. Sheng, and F. D. M. Haldane, Phys. Rev. Lett. **97**, 036808 (2006).
[33] E. Prodan, Phys. Rev. B **80**, 1 (2009).
[34] Y. Yang, Z. Xu, L. Sheng, B. Wang, D. Xing, and D. Sheng, Phys. Rev. Lett. **107**, 066602 (2011).
[35] L. Sheng, H.-C. Li, Y.-Y. Yang, D.-N. Sheng, and D.-Y. Xing, Chin. Phys. B **22**, 067201 (2013).
[36] Z. Qiao, S. A. Yang, W. Feng, W.-K. Tse, J. Ding, Y. Yao, J. Wang, and Q. Niu, Phys. Rev. B **82**, 161414 (2010).
[37] C. Fang, M. J. Gilbert, and B. A. Bernevig, Phys. Rev. B **86**, 115112 (2012).
[38] C.-C. Liu, H. Jiang, and Y. Yao, Phys. Rev. B **84**, 195430 (2011).
[39] M. Ezawa, Phys. Rev. Lett. **109**, 055502 (2012).
[40] S.-T. Wu and C.-Y. Mou, Phys. Rev. B **67**, 024503 (2003).
[41] S. B. Chung and R. Roy, Phys. Rev. B **90**, 224510 (2014).
[42] P. D. Sacramento, M. A. N. Araújo, and E. V. Castro, EPL (Europhysics Letters) **105**, 37011 (2014), arXiv:1302.3122 [cond-mat.supr-con].
[43] N. Read and D. Green, Phys. Rev. B **61**, 10267 (2000), arXiv:9906453 [cond-mat].
[44] T. Qin, Q. Niu, and J. Shi, Phys. Rev. Lett. **107**, 236601 (2011).
[45] H. Sumiyoshi and S. Fujimoto, J. Phys. Soc. Japan **82**, 1 (2013).